Biomaterials 32 (2011) 8797–8805

Contents lists available at SciVerse ScienceDirect

Biomaterials

journal homepage: www.elsevier.com/locate/biomaterials

Selective adhesion and growth of vascular endothelial cells on bioactive peptide nanofiber functionalized stainless steel surface

Hakan Ceylan, Ayse B. Tekinay**, Mustafa O. Guler*

UNAM-Institute of Materials Science and Nanotechnology, Bilkent University, Ankara 06800, Turkey

ARTICLE INFO

Article history:
Received 21 July 2011
Accepted 8 August 2011
Available online 31 August 2011

Keywords:
Stent
Endothelialization
Peptide
Self assembly
ECM (extracellular matrix)
Biomimetic materials

ABSTRACT

Metal-based scaffolds such as stents are the most preferred treatment methods for coronary artery disease. However, impaired endothelialization on the luminal surface of the stents is a major limitation occasionally leading to catastrophic consequences in the long term. Coating the stent surface with relevant bioactive molecules is considered to aid in recovery of endothelium around the wound site. However, this strategy remains challenging due to restrictions in availability of proper bioactive signals that will selectively promote growth of endothelium and the lack of convenience for immobilization of such signaling molecules on the metal surface. In this study, we developed self-assembled peptide nanofibers that mimic the native endothelium extracellular matrix and that are securely immobilized on stainless steel surface through mussel-inspired adhesion mechanism. We synthesized Dopa-conjugated peptide amphiphile and REDV-conjugated peptide amphiphile that are self-assembled at physiological pH. We report that Dopa conjugation enabled nanofiber coating on stainless steel surface, which is the most widely used backbone of the current stents. REDV functionalization provided selective growth of endothelial cells on the stainless steel surface. Our results revealed that adhesion, spreading, viability and proliferation rate of vascular endothelial cells are remarkably enhanced on peptide nanofiber coated stainless steel surface compared to uncoated surface. On the other hand, although vascular smooth muscle cells exhibited comparable adhesion and spreading profile on peptide nanofibers, their viability and proliferation significantly decreased. Our design strategy for surface bio-functionalization created a favorable microenvironment to promote endothelial cell growth on stainless steel surface, thereby providing an efficient platform for bioactive stent development for long term treatment of cardiovascular diseases.

1. Introduction

The World Health Organization describes cardiovascular diseases as number one cause of death globally. Currently, stent implantation is the most widely used method of performing coronary intervention because of its immediate success in preventing acute vessel closure and elastic recoil following balloon angioplasty [1]. However, in the long term, the risks of restenosis and in-stent thrombosis limit the ultimate success and ubiquitous use of this technology [2–5]. In order to improve the effectiveness of stents and to overcome the challenges associated with their use, a number of optimization strategies have been employed. Conventional drug-eluting stents and biodegradable stents are among these efforts. Drug eluting stent technologies slowly release anti-proliferative drugs to inhibit the proliferation of smooth muscle cells and they have been a breakthrough strategy to reduce the rate of in-stent restenosis [6,7]. Nevertheless, since anti-proliferative role of the drugs delay endothelialization, blood is exposed to the stent struts and/or to the surface coating, markedly increasing the propensity of thrombosis [8,9]. Delayed or impaired endothelialization also limits the long-term success against restenosis [9,10].

Endothelial cells are responsible for proper functioning of the coronary arteries, tightly controlling the migration and proliferation of smooth muscle cells, and inhibiting platelet activation inside the blood. Rapid recovery of endothelium at the coronary intervention site is, therefore, considered to be a critical factor in the healing process of the arterial walls. For this reason, an optimal cardiovascular therapy should target selective growth of endothelium on the stent surface, rather than ubiquitously blocking the

* Corresponding author. Tel.: +90 312 290 3552; fax: +90 312 266 4365.
** Corresponding author. Tel.: +90 312 290 3572; fax: +90 312 266 4365.
E-mail addresses: atekinay@unam.bilkent.edu.tr (A.B. Tekinay), moguler@unam.bilkent.edu.tr (M.O. Guler).

0142-9612/$ – see front matter © 2011 Elsevier Ltd. All rights reserved.
doi:10.1016/j.biomaterials.2011.08.018

growth of all residual cells by administering a number of toxins within the arteries. For this purpose, mimicking the native tissue properties to promote re-formation of endothelium will be the most advantageous strategy to succeed in the long-term treatment of cardiovascular diseases. The conventional stent technologies largely lack this bio-functionality for selective promotion of endothelial growth.

In the present study, we developed a bioactive stent coating that provides endothelial cells selective advantages in adhesion, spreading, viability and proliferation on stainless steel surface, which is the most widely used backbone material of the coronary stents. Our coating design is composed of three basic components that are equally critical for optimal functionalization of the metal surface in order to promote endothelialization. First component is a bioactive element that mediates endothelial cell specific adhesion, spreading and growth. For this purpose, we utilized a peptide amphiphile (PA) molecule with REDV sequence derived from the alternatively-spliced IIICS-5 fibronectin domain. The REDV epitope is recognized by $\alpha_4\beta_1$ integrins [11,12] and had been reported to selectively promote endothelial cell adhesion and spreading over smooth muscle cells and platelets [11,12]. Second component includes a Dopa molecule which is a biocompatible biological adhesive element for efficient immobilization of bioactive molecules on metal surfaces. Dopa (3,4-dihydroxyphenyl-L-alanine) is highly enriched in mussel-adhesive system to attach the mussel body onto almost any kind of inorganic or organic surface [13] by forming strong hydrogen bonds with hydrophilic surfaces and very strong complexes with metal ions and metal oxides [14–16]. Despite strong and non-covalent adhesive character, Dopa adhesion is fully reversible [14]. With such unique properties, Dopa-mediated adhesion system offers outstanding potential in surface functionalization of metals with a wide variety of biological molecules. The third component, peptide amphiphile nanofibers, is the backbone platform that will mimic the native extracellular matrix in terms of structure and biology by presenting the bioactive REDV signal, with an optimal geometry and ligand density. By bringing together the architecture and function of extracellular matrix, self-assembled PA nanofibers sustain cell–matrix interactions at the molecular level with end results including cellular adhesion, spreading, proliferation and differentiation [17–19]. In addition, PA nanofiber scaffolds can provide both instructive cues and mechanical support to the developing tissue [17,18,20]. Therefore, we designed and synthesized two self-assembling PA molecules; one functionalized with REDV peptide sequence and the other with a Dopa residue (Fig. 1). Upon their self-assembly, catechol groups of Dopa residues on the nanofibers formed surface adsorption, while REDV signals mediated endothelial cell specific bioactivity (Fig. 1d). We analyzed adsorption of PA nanofibers and characterized surface properties of the nanofibrous network adsorbed on stainless steel surface. *In vitro* adhesion, spreading, viability and proliferation of vascular endothelial and smooth muscle cells on the nanofibers coated on stainless steel surface were characterized. We further investigated platelet attachment on the nanofibers coated on stainless steel surface.

2. Materials and methods

2.1. Materials

9-Fluorenylmethoxycarbonyl (Fmoc) and other protected amino acids, lauric acid, [4-[α-(2′,4′-dimethoxyphenyl) Fmoc-amino methyl] phenoxy] acetomido-norleucyl-MBHA resin (Rink amide MBHA resin), 2-(1H-Benzotriazol-1-yl)-1,1,3,3-tetramethyluroniumhexafluorophosphate (HBTU) and diisopropylethylamine (DIEA) were purchased from Merck and ABCR. 100–200 mesh Wang resin was purchased from NovaBiochem and valine was loaded onto it for Fmoc-Val-Wang resin. Stainless steel, cover glass (15 mm Φ) and tissue culture plates (24-well) were purchased from Small Parts, Deckglaser, and BD, respectively. All other chemicals and materials used in this study were analytical grade and obtained from Invitrogen, Fisher, Merck, Alfa Aesar, and Sigma–Aldrich.

2.2. Synthesis and characterization of peptide amphiphiles (PA)

Functionalized PA molecules were synthesized manually by standard solid phase Fmoc peptide synthesis chemistry. REDV-PA (C12-VVAGEREDV) and E-PA (C12-VVAGE) were synthesized on Fmoc-Val-Wang and Fmoc-Glu-Wang resins,

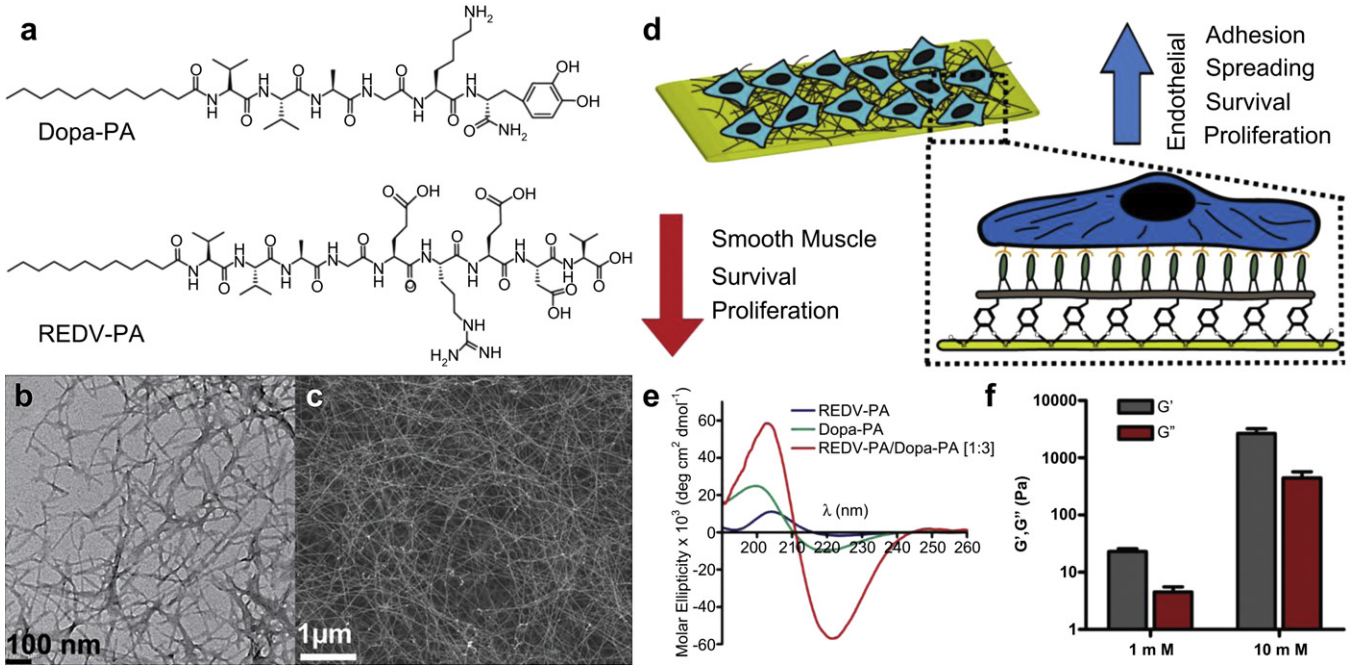

Fig. 1. (a) Design and chemical representation of PA molecules. TEM (b) and SEM (c) images revealed the nanofibrous network that mimic the native matrix architecture. (d) Schematic representation of REDV-PA/Dopa-PA network, which is designed to functionalize stainless steel surface to support endothelial cell adhesion, spreading, viability and proliferation. (e) Circular dichroism results revealed formation of β-sheet structure, which drives nanofiber formation upon mixing Dopa-PA and REDV-PA at physiological pH. (f) Rheology results showed gelation as a result of nanofibrous network formation by Dopa-PA and REDV-PA at pH 7.4.

respectively. Dopa-PA (C12-VVAGKDopa-Am) and K-PA (C12-VVAGK-Am) were synthesized on Rink amide resins. Amino acid couplings were performed with 2 equivalents of amino acids activated with 1.95 equivalents of HBTU, and 3 equivalents of DIEA for 1 equivalent of starting resin. Coupling time for each amino acid was 2 h. Lauric acid addition was performed similarly to amino acid coupling except that coupling time was 4 h. Fmoc removal was performed with 20% piperidine/dimethylformamide (DMF) solution for 20 min. 10% acetic anhydride/DMF solution was used to permanently acetylate the unreacted amine groups after each coupling step. DMF and dichloromethane (DCM) were used as washing solvents. Cleavage of protecting groups and peptide molecules from the resin was carried out by 95% trifluoroacetic acid-containing cleavage cocktail (95% TFA, 2.5% water, 2.5% triisopropylsilane) for 3 h. Excess TFA removal was carried out by rotary evaporation. PAs in the remaining solution were precipitated in ice-cold diethyl ether overnight. The precipitate was collected next day by centrifugation and dissolved in ultra pure water. This solution was frozen at −80 °C for 4 h and then lyophilized for one week. Synthesis of PAs were characterized by Agilent 6530 quadrupole time of flight (Q-TOF) mass spectrometry with electrospray ionization (ESI) source equipped with reverse-phase analytical high performance liquid chromatography (HPLC) with Zorbax Extend-C18 2.1 × 50 mm column for basic conditions and Zorbax SB-C8 4.6 × 100 mm column for acidic conditions. An optimized gradient of 0.1% formic acid/water and 0.1% formic acid/acetonitrile for acidic conditions and 0.1% ammonium hydroxide/water and 0.1% ammonium hydroxide/acetonitrile for basic conditions were used as mobile phase for analytical HPLC, respectively. A reverse-phase preparative-HPLC (Agilent 1200 series) system was employed for purification of REDV-PA by using Zorbax Extend-C18 21.2 × 150 mm column. Residual TFA was removed from positively-charged Dopa-PA by 0.1% HCl treatment. All lyophilized PA samples were reconstituted in 20 mM HEPES buffer at pH 7.4 for further use.

2.3. Self-assembled nanofibrous network formation

Nanofibers were formed by mixing negatively-charged REDV-PA and positively-charged Dopa-PA at pH 7.4 at 1:3 ratio, respectively. For Dopa control, REDV-PA and K-PA were mixed to form REDV-PA/K-PA nanofibers at pH 7.4 at 1:3 ratio, respectively. For REDV control, E-PA and Dopa-PA were mixed to form E-PA/Dopa-PA nanofibers at pH 7.4 at 1:2 ratio, respectively. These ratios were used to balance the charges on mixing PA molecules. To visualize nanofibers and the resulting network formation, scanning electron microscopy (SEM) and transmission electron microscopy (TEM) were employed. SEM samples were prepared on cleaned stainless steel surface by mixing 1 mM REDV-PA and Dopa-PA at 1:3 ratio, respectively. Following 10 min of gelation, the hydrogel was dehydrated in gradually increasing concentrations of ethanol solutions. The dehydrated hydrogel was dried with a Tourismis Autosamdri®-815B critical-point-drier to preserve the network structure. The dried samples were coated with 3 nm Au/Pd and visualized under high vacuum with a FEI Quanta 200 FEG scanning electron microscope equipped with ETD detector. TEM images were acquired with FEI Tecnai G2 F30 TEM at 300 kV. Samples for TEM were prepared by mixing 1 mM REDV-PA and Dopa-PA at 1:3 ratio, respectively, on a 200-mesh carbon TEM grid for 3 min followed by 2 wt% uranyl-acetate staining for 1 min and drying immediately under nitrogen gas. Formation of network structure at pH 7.4 was also validated by using oscillatory rheology. An Anton Paar Physica RM301 Rheometer operating with a 25 mm parallel plate configuration was used to probe the viscoelastic properties of the PA networks. Samples of both 1 mM REDV-PA and Dopa-PA or 10 mM REDV-PA and Dopa-PA were mixed on the lower stage of the rheometer at 1:3 ratio, respectively, and allowed for gelation for 10 min before the measurements. A gap distance of 0.5 mm was used with 10 rad/s angular frequency and 0.1% shear strain. To investigate the secondary structure of PA nanofibers, circular dichroism (CD) spectra of 1×10^{-5} M REDV-PA, 3×10^{-5} M Dopa-PA and their mixture at these concentrations at pH 7.4 were measured at room temperature from 260 nm to 190 nm with 0.1 nm data interval and 500 nm/min scanning speed. The results were converted to and represented as the mean residue ellipticity, θ. Zeta potential measurements were performed with a Malvern Zeta-ZS Zetasizer using individual PA solutions or their mixture at ratios and $1{:}10^{-6}$ concentrations indicated above.

2.4. Adsorption analysis and surface characterization of PA nanofibers on stainless steel

The adsorption behavior of PA nanofibers on stainless steel surface was assessed by X-ray photoelectron spectroscopy (XPS), attenuated total internal reflectance Fourier transform infrared spectroscopy (ATR-FT-IR), contact angle measurements, and SEM. 1 mM REDV-PA and Dopa-PA (or REDV-PA/K-PA nanofibers were formed as a control for Dopa activity) solutions were mixed on cleaned stainless steel surface at 1:3 ratio, respectively. In order to prevent solvent evaporation and thus to ensure adsorption in the presence of water, the samples were kept in a humidified environment for 24 h at room temperature. The substrates were then rinsed in water for half an hour with agitation, and dried at 37 °C for a further period of 24 h. In order to characterize the chemical composition and the molecular structure of the film formed on the surface upon drying; XPS and FT-IR spectra were acquired on the surface. A Thermo Scientific XPS spectrometer with Al-Ka monochromatic (100–400 eV range) X-ray source and ultra-high vacuum ($\sim 10^{-9}$ Torr) was employed to identify the chemical composition of the surface. The spectra were acquired from at least three random locations on the surface. VORTEX 70 Fourier transform infrared spectrometer equipped with liquid nitrogen-cooled MCT detector was utilized to identify the FT-IR spectrum of the surface by using a germanium ATR objective. The spectrum range was between 4000 and 400 cm^{-1}. The spectra were acquired from at least three different locations on the surface. The change in the surface hydrophilicity was probed by an OCA 30 Data physics contact angle meter to measure the static water contact angles on the stainless steel surface before and after adsorbed PA nanofibers. 4 μL water droplets were used with Laplace–Young fitting for contact angle measurements. The thickness of the adsorbed surface coatings was evaluated using a Zygo New view 7200 optical profilometer. Surface roughness was analyzed by atomic force microscope (AFM) and optical profilometer. An AFM from Asylum Research was employed to scan at least three different locations of REDV-PA/Dopa-PA coated stainless steel surface from the in an area of 103.3–458.4 μm^2 in tapping mode. The spring constant was 40 N/m with a resonant frequency of 245 kHz. Adsorbed peptide nanofibers on stainless steel were visualized using SEM. Samples were prepared by dehydrating the coating after the washing in gradually increasing concentrations of ethanol solutions. The dehydrated sample was dried with a Tourismis Autosamdri®-815B critical-point-drier. The dried samples were coated with 3 nm Au/Pd and visualized under high vacuum with a FEI Quanta 200 FEG scanning electron microscope equipped with ETD detector.

2.5. PA-coated surface preparation for in vitro characterizations

In order to elucidate the impact of functionalized PA nanofibers on vascular cells, cleaned stainless steel, glass and tissue culture plates were prepared by coating with PA nanofibers. Stainless steel surfaces were cleaned by using ultrasonic cleaning in acetone, ethanol and ultra pure water, for 1 h each, sequentially. The cleaned surfaces were kept in a vacuum oven at 90 °C for 4 h to completely evaporate the residual water. Glass and tissue culture plate surfaces were used as received. Stainless steel, glass and tissue culture plate surfaces were coated with PA nanofibers by drop-casting method. 1 mM REDV-PA and 1 mM Dopa-PA solutions were mixed on the surfaces at 1:3 ratio, respectively. The coated surfaces were first air-dried in a chemical hood overnight. The substrates were further dried at 37 °C for 24 h. Sterilization of the coated substrates was carried out by UV irradiation for 2–3 h. All coated surfaces were washed with PBS for ~15 min prior to the experiments.

2.6. Cell culturing and maintenance

Adhesion, spreading, viability and proliferation behaviors of vascular cells on REDV-PA/Dopa-PA nanofibers were characterized by using human umbilical vein endothelial cells (HUVECs), A7r5 rat aortic smooth muscle cells (ATCC® Cat# CRL-1444™) and A10 rat aortic smooth muscle cells (ATCC® Cat# CRL-1476™). HUVECs were donated by Yeditepe University, Istanbul, Turkey. HUVECs were purified as described [21] and characterized by staining with CD34, CD31, and CD90 surface markers. These cells were found to be positive for CD31 and CD34 but negative for CD90. HUVECs and A10 cells were cultured in 75 cm^2 polystyrene cell culture flasks with 10% fetal bovine serum (FBS), 2 mM L-glutamine and 1% penicillin/streptomycin containing Dulbecco's modified eagle medium (DMEM). A7r5 cells were grown in 10% fetal calf serum (FCS), 2 mM L-glutamine and 1% penicillin/streptomycin containing DMEM. All *in vitro* experiments and passaging were carried out at cell confluence between 80 to 90% using trypsin/EDTA chemistry. Cells were diluted 1:2 and 1:3 for splitting.

2.7. Adhesion, spreading and cytoskeleton analysis of vascular cells on PA-coated surfaces

Early adhesion of HUVEC, A7r5 and A10 cells were analyzed on PA-coated stainless steel surfaces after 2 h of incubation. PA-coated glass and tissue culture plate surfaces were also used to evaluate the adhesion of the cells on different surfaces. Prior to adhesion experiments, HUVEC, A10 and A7r5 cells were incubated with serum-free DMEM medium supplemented with 4 mg/ml BSA and 50 μg/ml cyclohexamide for 1 h at standard cell culture conditions (37 °C, 5% CO_2 and 95% humidity). Then the cells were seeded onto the surfaces with serum-free DMEM at densities of 3×10^4, 1.5×10^4, and 1.5×10^4 cells/cm^2, respectively. The cells were incubated at standard cell culture conditions for 2 h. After 2 h, the unbound cells were washed away with PBS, and the remaining bound cells were stained with 1 μM Calcein AM (Invitrogen). Relative cell adhesions were quantified by counting the number of cells on different locations (at least 4 different locations per surface, i.e., at least 36 photographs per type of surface, such as "REDV-PA/Dopa-PA coated stainless steel surface", were acquired) of the surface using a fluorescent microscope. The total number of cells was averaged for each type of surface (i.e., coated stainless steel, bare glass, etc) and normalized to bare surfaces to evaluate the relative cell adhesion. Spreading and cytoskeletal organization of vascular cells were analyzed on PA coated stainless steel surface at 2 h, 24 h and 72 h. Samples to be analyzed at 2 h were prepared similarly to cell adhesion experiment. Preparation of the sample to be analyzed at 24 h was the same as the sample for the viability assay and preparation of the sample to be analyzed at 72 h was the same as the sample for the proliferation assay except that no EdU was added into the medium. After these time intervals, i.e. 2 h, 24 h and 72 h later, cells were fixed with 3.7% formaldehyde for 15 min and permeabilized in 0.1% Triton X-100 for 10 min. Filamentous actins were stained with TRITC-conjugated phalloidin and the cell nuclei were stained with

TO-PRO®-3 iodide. The samples were analyzed with Zeiss LSM 510 confocal microscope. Cell spreading was quantified by measuring cell diameters on the equipment's software, ZEN 2008. HUVEC-matrix interactions were investigated using scanning electron microscopy. HUVECs were seeded on PA coated stainless steel surface in the same manner described in the sample preparation for the cell adhesion experiments. Following 2 h incubation, HUVECs were fixed with 2% gluteraldehyde and 4% osmium tetroxide solutions at room temperature for 1 h each, sequentially. The samples were then dehydrated in increasing concentrations of ethanol and dried with Tourismis Autosamdri®-815B critical point drier to preserve cellular and nanofibrous structures. The samples were coated with 4 nm Au/Pd and analyzed by using FEI Quanta 200 FEG scanning electron microscope equipped with ETD detector under high vacuum.

2.8. Viability and proliferation of vascular cells on PA nanofibers

Viability and proliferation of HUVEC, A7r5, and A10 cells were analyzed on PA-coated stainless steel surface at 24 h and 72 h, respectively. Coated glass and tissue culture plate surfaces were also used to evaluate the viability of the cells on different surfaces. Cells were seeded onto PA coated stainless steel, glass and tissue culture plate surfaces with DMEM media supplemented with 10% FBS (for HUVECs and A10 cells) or 10% FCS (for A7r5 cells), 2 mM L-glutamine, and 1% penicillin/streptomycin at densities of 1.5×10^4, 0.75×10^4 and 0.75×10^4 cells/cm^2, respectively. Cells were incubated at standard tissue culture conditions for 24 h. After 24 h, cells were washed with and then stained with 1 μM Calcein AM. Viability of the cells on PA coated surfaces was quantified by counting the number of live cells in images taken with a fluorescence microscope. The total count of live cells was normalized to bare surfaces to evaluate the relative viability. In order to evaluate cell proliferation on PA coated stainless steel, Click-iT™ EdU assay was utilized. Vascular cells were incubated with a nucleoside analog of thymine, EdU (5-ethynyl-2′-deoxyuridine), in their cell culture media. EdU incorporates in DNA during the synthesis phase (S phase) of the cell cycle and thus enables direct quantification of proliferation. HUVEC, A10, and A7r5 cells were seeded on the steel surfaces with DMEM media supplemented with 10% FBS (for HUVECs and A10 cells) or 10% FCS (for A7r5 cells), 2 mM L-glutamine, and 1% penicillin/streptomycin, at a density of 5×10^3 cells/cm^2. Bare stainless steel surface served as a negative control. After the initial 8 h incubation upon seeding, cell medium was replaced with 10 μM EdU-containing DMEM media supplemented with 10% FBS (HUVECs and A10 cells) or 10% FCS (A7r5 cells), 2 mM L-glutamine, and 1% penicillin/streptomycin. Cells were incubated at standard cell culture conditions for another 72 h. Cells were then fixed with 4% formaldehyde, permeabilized in 5% Triton X-100 and treated with Alexaflour-488 conjugated azide in accordance with the recommendation of the supplier. Proliferation rates of the cells were quantified upon the staining of nuclei. Using a fluorescent microscope, the average counts of stained cell nuclei were used to evaluate the relative rates of proliferation.

2.9. Platelet adhesion on PA nanofibers

The protocol used to evaluate platelet adhesion on PA coated stainless steel surface was derived from a previous report [19]. Whole blood from a healthy volunteer was collected into BD Vacutainer® EDTA K2E tubes and then mixed with Quinacrine dihydrochloride to label platelets. Collagen I-coated stainless steel surface served as positive control and the bare metal surface served as negative control. 2.5 mg/ml collagen I prepared in 3% glacial acetic acid was coated on stainless steel surface in the same manner described in PA coating. Blood samples were incubated on each surface for 2 h at 37 °C. Platelet attachment was quantified by acquiring 5 random images on each surface at 10× magnification by using a fluorescent microscope. Average numbers of adhered platelets were used to evaluate the relative attachment of platelets onto the surfaces.

2.10. Statistical analysis

Unless otherwise indicated, all the quantitative results were expressed as mean ± standard error of means (s.e.m.). All *in vitro* experiments were quantified with at least 4 replicates and with at least 3 independent repeats. All surface characterizations were carried out with at least 3 independent repeats. Statistical analyses were carried out by either one-way analysis of variance (ANOVA) or Student's *t*-test. A *p*-value less than 0.05 was considered statistically significant.

3. Results and discussion

3.1. Synthesis of PA molecules and characterization of their self-assembly into nanofibers

REDV-PA and Dopa-PA molecules were designed (Fig. 1a) and synthesized for functionalization of stainless steel surfaces. REDV-PA was designed to enhance endothelial cell specific activity, including adhesion, spreading, survival and proliferation. Under flow conditions in blood, growing endothelium will feel resistance to attach to the struts of the stent or to the polymer coatings, where anti-proliferative toxin release might double the difficulty. The advantage of REDV over other popular binding sequences, such as RGD or YIGSR, is the selectivity of this ligand toward endothelial cells [11,12]. Unlike REDV, other bio-adhesive sequences also attract platelets [22]. The rationale behind Dopa incorporation into the PA design was to immobilize REDV-conjugated fibers on the implant surface. In order to assess the specific function of Dopa and REDV, K-PA and E-PA, respectively, were synthesized (Fig. S1). REDV-PA and Dopa-PA molecules were mixed at 1:3 ratios, respectively, to form a homogenous nanofibrous network, where all the charges are balanced. Niece *et al.* previously showed that two oppositely charged PA molecules attract each other via electrostatic interactions and thus can be homogenously mixed to form heterogeneous peptide nanofibers at physiological pH [23]. To support homogenous mixing of REDV-PA and Dopa-PA into heterogeneous nanofibers, we employed circular dichroism technique. CD results revealed that when Dopa-PA and REDV-PA are in solution, their β-sheet forming capacity is limited based on the magnitude of molar ellipticity (Fig. 1e). However, upon mixing, their combined capacity of β-sheet formation becomes much greater than the sum of the individual fibers. This showed that emerging salt bridges between oppositely charged PA molecules stabilize them to drive nanofiber formation. Zeta potential measurements supported self-assembly process as mixing two oppositely charged PA molecules reduced the stability of the mixture between −30/+30 mV (Fig. S7). Transmission electron microscopy (TEM) and scanning electron microscopy (SEM) images revealed the porous and nano-scale architecture formed by REDV-PA/Dopa-PA that recapitulated the structure of native extracellular matrix (Fig. 1b, c). Rheology measurements indicated formation of a hydrogel ($G' > G''$) at both 1 mM and 10 mM concentrations of PA mixtures even within 10 min at pH 7.4 (Fig. 1f). This result further confirmed the formation of a scaffold formed by the self-assembled REDV-PA/Dopa-PA nanofibers at physiological pH.

3.2. Adsorption analysis and surface characterizations of the nanofibers on stainless steel surface

Adsorption of REDV-PA/Dopa-PA nanofibers onto stainless steel surface was primarily inspected by XPS, FT-IR, and SEM techniques. The primary reason for choosing stainless steel for adsorption study is that most of the currently available coronary stents are made out of stainless steel, primarily due to its exceptional biocompatibility [24]. The complete suppression of photoelectron peaks of iron (Fe 2p) and chromium (Cr 2p) from the stainless steel surface and the emergence of a new nitrogen (N 1s) peak along with increased carbon (C 1s) peak after the washing were considered as evidence for the permanent adsorption of REDV-PA/Dopa-PA nanofibers (Fig. 2a). We observed that the thickness of the coating is around 1.27 ± 0.22 μm (Table S1) according to optical profilometer measurements. In addition, as shown in Fig. S2a, nearly half of the adsorbed nanofibrous coating of REDV-PA/Dopa-PA was retained on the surface even after 2 h of ultrasound sonication in water. In order to verify that the adsorption was mainly Dopa-mediated, but not due to simple electrostatic interactions between PA nanofibers and the steel surface, we formed peptide nanofibers by mixing REDV-PA and K-PA molecules at pH 7.4 at 1:3 ratios, respectively. In this construct, the nanofibers were functionalized with bioactive REDV peptide, but did not contain Dopa residue. Under the same washing conditions, REDV-PA/K-PA poorly attached onto the steel surface and did not form a peptide layer (Fig. 2a). These observations emphasize the critical role of Dopa in adhesion of nanofibers onto the stainless steel surface for convenient surface

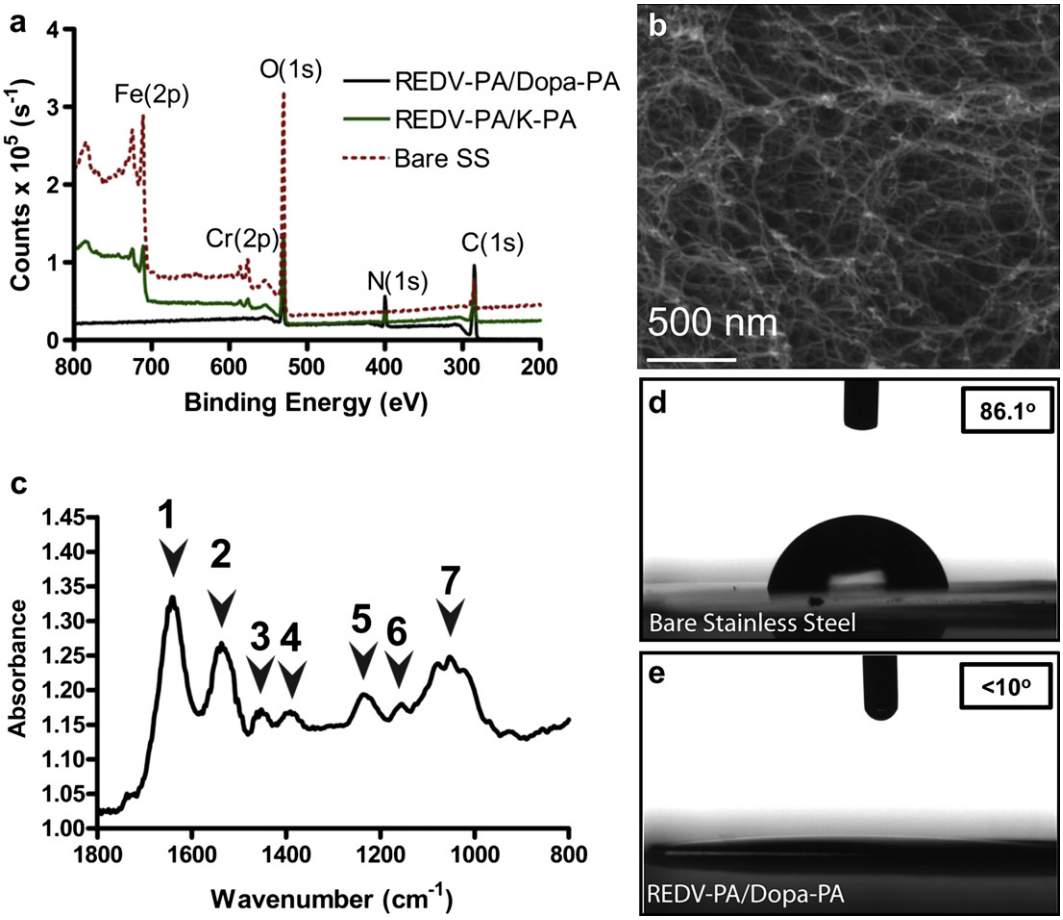

Fig. 2. Adsorption of REDV-PA/Dopa-PA nanofibers on stainless steel surface alters the surface characteristics. (a) XPS spectra of REDV-PA/Dopa-PA, REDV-PA/K-PA adsorbed and bare stainless steel surfaces. (b) SEM micrographs acquired on the REDV-PA/Dopa-PA-adsorbed steel surface. (c) FT-IR spectra acquired on REDV-PA/Dopa-PA adsorbed surface. (d, e) The contact angle measurements on bare and REDV-PA/Dopa-PA adsorbed stainless steel surfaces.

functionalization. Using SEM, we further characterized and confirmed the adsorbent species in REDV-PA/Dopa-PA samples on stainless steel surface to be PA nanofibers (Fig. 2b). FT-IR spectrum of adsorbed REDV-PA/Dopa-PA nanofibers on stainless steel was found to be similar to the FT-IR spectrum of previously reported Mefp-1 protein adsorbed on ZnSe surfaces [15]. From this spectrum, amide I, amide II and Dopa-specific peaks could be clearly assigned (Fig. 2c; see *Supporting Information* file for all peak assignments). Change in the surface hydrophilicity due to the adsorbing peptide layer was investigated by contact angle measurements. The contact angle of the bare stainless steel surface was measured to be 86.0 ± 1° (Fig. 2d). The peptide layer radically decreased the contact angle value below 10° (Fig. 2e). This can be explained by the highly porous and hydrophilic surface characteristics manifested by the outer surfaces of adsorbent PA nanofibers.

3.3. Characterization of the cellular responses on peptide nanofibers

Adhesion and spreading are the first events of cellular response to a substrate. In their native microenvironment, cells adhere to and interact with extracellular matrix proteins and other constituents through focal adhesions and other receptor-mediated interactions that govern a number of physiological responses including survival, proliferation and differentiation. REDV is an endothelial cell specific adhesive ligand found in the alternatively-spliced IIICS-5 domain of human plasma fibronectin [11,12]. This epitope was reported to mediate cell adhesion and spreading through α4β1 integrin in endothelial cells, but not in smooth muscle cells and fibroblasts [11,12]. By functionalizing PA nanofibers with this ligand, we aimed to create a microenvironment that imitates native matrix but selectively favors endothelium growth. For these reasons, the ability of PA nanofibers to functionally mimic native extracellular matrix was evaluated by analyzing first early adhesion and spreading of vascular cells on REDV-PA/Dopa-PA coated steel surfaces. Early adhesion and spreading experiments were carried out under serum-free conditions in order to avoid the interference of soluble ECM proteins found in the serum, to the observed behavior. Similarly, any unbound PA nanofibers were removed from the coated surface by PBS washing in order to prevent their interference into biological activity when they are in solution. In addition, the interference of endogenous proteins was minimized with a pre-treatment of BSA and cyclohexamide, a known translation inhibitor. Our results indicate that adhesion of HUVECs on REDV-PA/Dopa-PA coated surface was increased more than 7 folds compared to bare steel surface at 2 h (Fig. 3a, c, d). Similar trends were observed on coated glass and tissue culture plate surfaces (Fig. S3a). Despite such noteworthy increase in adhesion of HUVECs on REDV-functionalized PA nanofibers, there was no significant difference in adhesion of A7r5 vascular smooth muscle cells at 2 h on PA coated or uncoated stainless steel (Fig. 3d) and glass (Fig. S3c) surfaces. Moreover, a relatively slight (~0.2 fold) decrease in adhesion of these cells was observed on tissue culture plate surfaces when coated with REDV-PA/Dopa-PA nanofibers at 2 h

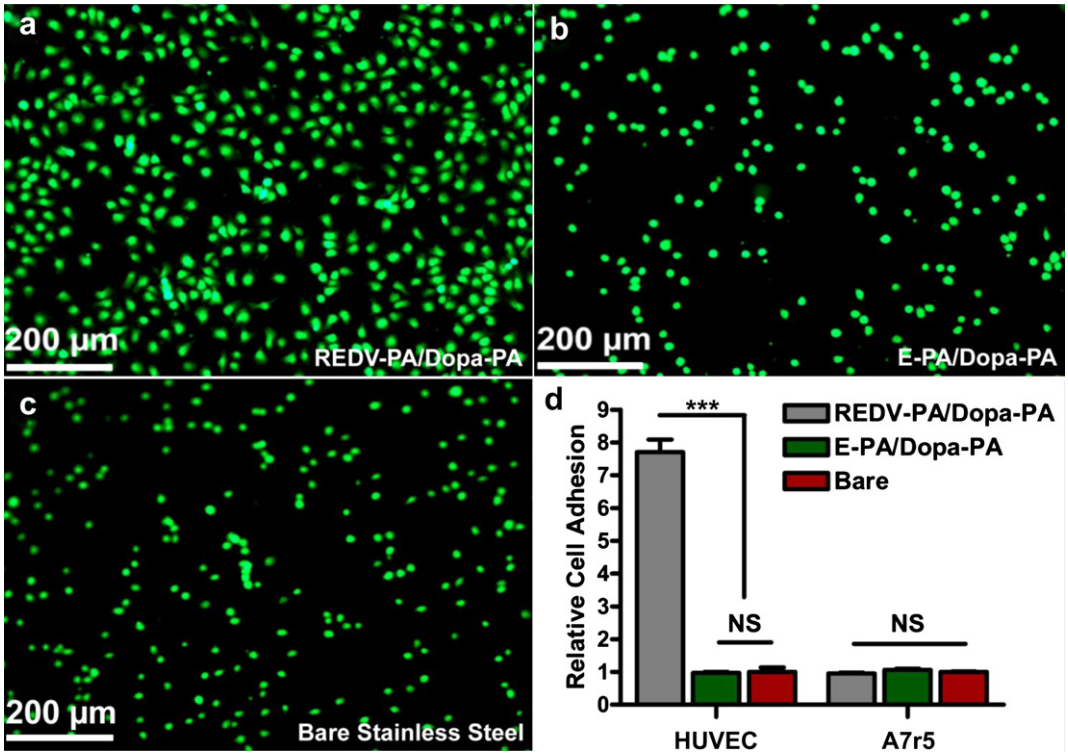

Fig. 3. Representative Calcein AM stained fluorescent images of HUVECs adhered on the stainless steel surfaces coated with REDV-PA/Dopa-PA nanofibers (a), E-PA/Dopa-PA nanofibers (b), and on the bare steel surface (c) at 2 h. (d) The relative adhesion of HUVECs and A7r5 smooth muscle cells on REDV-PA/Dopa-PA and E-PA/Dopa-PA coated surfaces with respect to the bare stainless steel surface at 2 h ***$p < 0.0001$, NS: No Significance.

(Fig. S3c). Similar to A7r5 cells, A10 vascular smooth muscle cells showed a comparable adhesion profile on REDV-PA/Dopa-PA and bare steel surface. (Fig. S5a) The selective bias of REDV-PA/Dopa-PA nanofibers toward endothelial cells in adhesion strength shows the critical role of REDV within this construct. To further verify this, we synthesized a negatively-charged PA molecule, E-PA, which can self-assemble with Dopa-PA but lacked REDV signal. E-PA was mixed with Dopa-PA at 1:2 ratios, to balance the charges and thus to drive nanofiber formation. The adhered number of HUVECs on E-PA/Dopa-PA coated stainless steel surface was reduced to a level comparable to the bare steel surface (Fig. 3b, c, d). In addition, adhered number of A7r5 cells was found to be insignificant between REDV-PA/Dopa-PA and E-PA/Dopa-PA coated steel surfaces (Fig. 3d). This crashing drop in the number of adhered HUVECs in the absence of REDV further underlies the crucial bioactivity and, more importantly, selectivity provided by this ligand in cell adhesion. By exploiting the sensitivity of HUVECs on REDV-PA/Dopa-PA, we qualitatively addressed the homogeneity of the REDV-PA/Dopa-PA coating and the reproducibility of the ligand density. As shown in Fig. S2b, fluorescent images of HUVECs from different locations of the stainless steel coated with REDV-PA/Dopa-PA were uniform in terms of adhered number of cells after at least three independent experiments and four replicates in each.

In parallel to the adhesion behavior, HUVECs showed improved spreading morphology on REDV-PA/Dopa-PA coated steel surfaces at 2 h than on bare stainless steel surface and on E-PA/Dopa-PA nanofibers (Fig. 4a–i). HUVECs gained their native morphology on REDV-PA/Dopa-PA within 2 h with an average cell diameter of 61.8 ± 1.19 μm. Their average cell area is almost 6 folds higher than HUVECs seeded on bare steel surface and nearly 3.5 folds higher than seeded on E-PA/Dopa-PA. HUVECs seeded on E-PA/Dopa-PA nanofibers had an average diameter of 31.9 ± 0.48 μm (nearly 1.7 folds of increase in cell area compared to the bare steel surface), again, highlighting the significance of REDV ligand for early spreading of endothelial cells on stainless steel surface. On the other hand, there was no significant difference in the average cell diameter of A7r5 cells seeded on neither REDV-PA/Dopa-PA nor on E-PA/Dopa-PA relative to bare metal surface (Fig. 4i). A10 vascular smooth muscle cells also showed no difference in spreading morphology and average diameter on between REDV-PA/Dopa-PA coated and bare steel surfaces (Fig. S5c). Overall, we demonstrate that REDV sequence on REDV-PA/Dopa-PA nanofiber network functions as a selective bioactive domain for endothelial cells by increasing their adhesion strength and spreading onto the stainless steel surface, two vital factors in the way of forming a monolayer inside the stent surface for functional regeneration.

After analyzing early adhesion and spreading of cells on REDV-PA/Dopa-PA coated stainless steel surface we sought to investigate the morphology, viability and proliferation of the vascular cells in the long term. Biocompatibility of surface coating in the long term period is an important parameter to evaluate the use of this coating. In this respect, HUVECs were observed to maintain their native morphology by forming actin stress fibers on REDV-PA/Dopa-PA coated stainless steel surface at 24 and 72 h (Fig. 5a, b, d, e). The viability of HUVECs at 24 h was found to be comparable on REDV-PA/Dopa-PA and E-PA/Dopa-PA coated and bare stainless steel surfaces (Fig. 5c). This result was also in agreement with viability of these cells on coated glass and tissue culture plates (Fig. S3b). Surprisingly, the viability of vascular smooth muscle cells was found to decrease sharply on both REDV-PA/Dopa-PA and E-PA/Dopa-PA coated surfaces with respect to bare steel surface. Viable A7r5 cell number decreased to 66 ± 2.3% on REDV-PA/Dopa-PA coated stainless steel surface with respect to bare stainless steel surface. This result was parallel on glass and tissue culture plate surfaces with 80.9 ± 3.9% and 73.9 ± 3.8% viability, respectively (Fig. S3d). It seems, however, that muscle cell viability was not

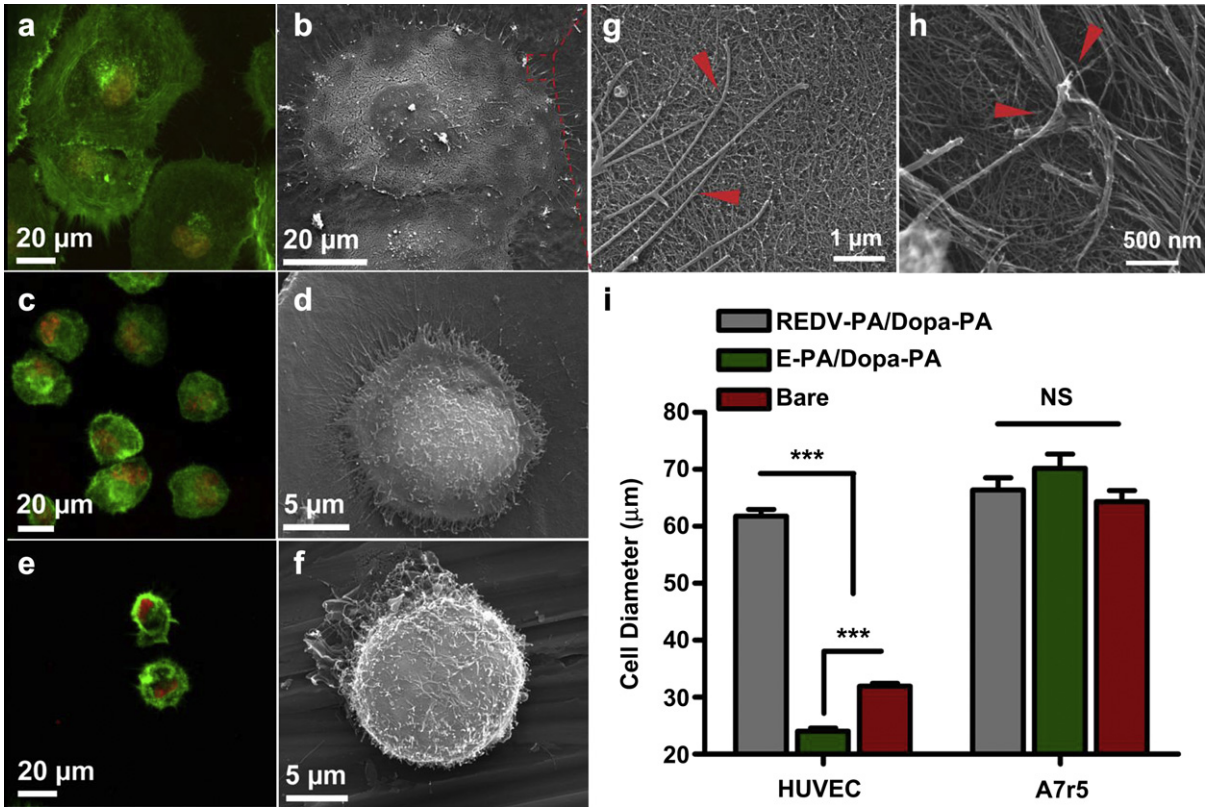

Fig. 4. Spreading of vascular cells on REDV-PA/Dopa-PA, E-PA/Dopa-PA coated and bare stainless steel surfaces. HUVECs spread and gained their morphology within 2 h on REDV-PA/Dopa-PA coated network (a, b) while these cells retained their rounded shape on stainless steel surface (b, d) and mostly on E-PA/Dopa-PA coated surface. The increase in the average cell diameter of HUVECs was more than two folds whilst the diameter of A7r5 cells remained the same on both PA coated and bare steel surfaces (g). Cells formed dynamic interactions with their surrounding PA nanofiber-based microenvironment. PA networks imitate the native extracellular matrix; HUVECs extend protrusions on the matrix within 2 h (as showed by arrows) (e) and exert force (f) to pull the network in accordance with their needs. a, c and e are confocal images. Green regions indicate filamentous actin stained with Phalloidin-TRITC, while red regions indicate the nucleus stained with TO-PRO®-3 iodide. b, d, f, g and h are SEM micrographs. ***$p < 0.0001$, NS: No Significance.

caused by REDV epitope as cells behaved similarly on both E-PA/Dopa-PA and REDV-PA/Dopa-PA at 24 h. We also observed apoptotic body-like structures of A7r5 cells on both REDV-PA/Dopa-PA and E-PA/Dopa-PA (Fig. S4). The viability of A10 cells demonstrated the same trend with an even sharper decrease (Fig. S5b). Overall, this trend of decrease in viability of smooth muscle cells on coated surfaces strengthens the idea that this coating provides an unfavorable environment for this cell type. On the other hand, increased adhesion and spreading of HUVECs with long term viability on REDV-PA/Dopa-PA coating favors endothelialization over the stainless steel surface. The adaptive and viable microenvironment provided by REDV-PA/Dopa-PA nanofibers also imparted a selective advantage for HUVECs to proliferate at a higher rate in the long term. Proliferation of HUVECs on this surface was found to increase by 16.9 ± 5.2% after 72 h compared to bare metal surface (Fig. 5f). This increase was also observed in E-PA/Dopa-PA coated steel surface with 18.3 ± 5.4%, revealing that REDV might not be responsible for the increased proliferation. The increase in proliferation of HUVECs might be due to the adaptive microenvironment provided by the nano-scale matrix through surface topography, hydrophilicity, and structure that mimics natural matrix. On REDV-PA/Dopa-PA, HUVECs attached and spread readily, thereby gaining a competitive advantage in this biomimetic microenvironment for proliferation to form a monolayer on the metal surface. In addition, PA coating on stainless steel increases hydrophilicity (Fig. 2d, e) and roughness (Fig. S6, Table S1) of the surface, which may dramatically influence the growth of these cells on this coating. The growth of HUVECs was previously shown to increase on nano-scale rough surfaces [25]. Proliferation rates of vascular smooth muscle cells were also in a similar trend with viability results. Relative rate of proliferation of A7r5 cells on REDV-PA/Dopa-PA coated metal surface was found to be 45.5 ± 2.8% of cells cultivated on bare metal and 50.0 ± 1.3% on E-PA/Dopa-PA coated steel surface of cells cultivated on bare surface (Fig. 5f). This profound decrease was also observed in A10 cells with a relative proliferation rate of 27.3 ± 1.3% of the bare steel surface (Fig. S5d). Despite the fact that muscle cells attached at comparable rates and spread in similar morphology on PA coated and bare metal surfaces, the viability and proliferation of these cells remarkably decreased at 24 h and 72 h. We also noticed that REDV signal might not be the key determinant for the differences in viability of HUVECs and A7r5 cells. We implicated that the lowered proliferation rates of A7r5 and A10 smooth muscle cells were the result of the unfavorable conditions that also cause lowered viability of these cells on the peptide nanofibers. Apart from potential receptor-mediated interactions, the physical and chemical factors including surface chemistry, topography, hydrophilicity and structural and mechanical properties of the nanofibrous network, provided by peptide nanofibers, collectively, are determining factors for the long term viability and proliferation of cells [26–28].

3.4. Platelet adhesion on PA nanofibers

Another major limitation of currently available vascular grafts is the risk of progression of late thrombosis. Since the main orientation of this study is to promote endothelialization on the stent

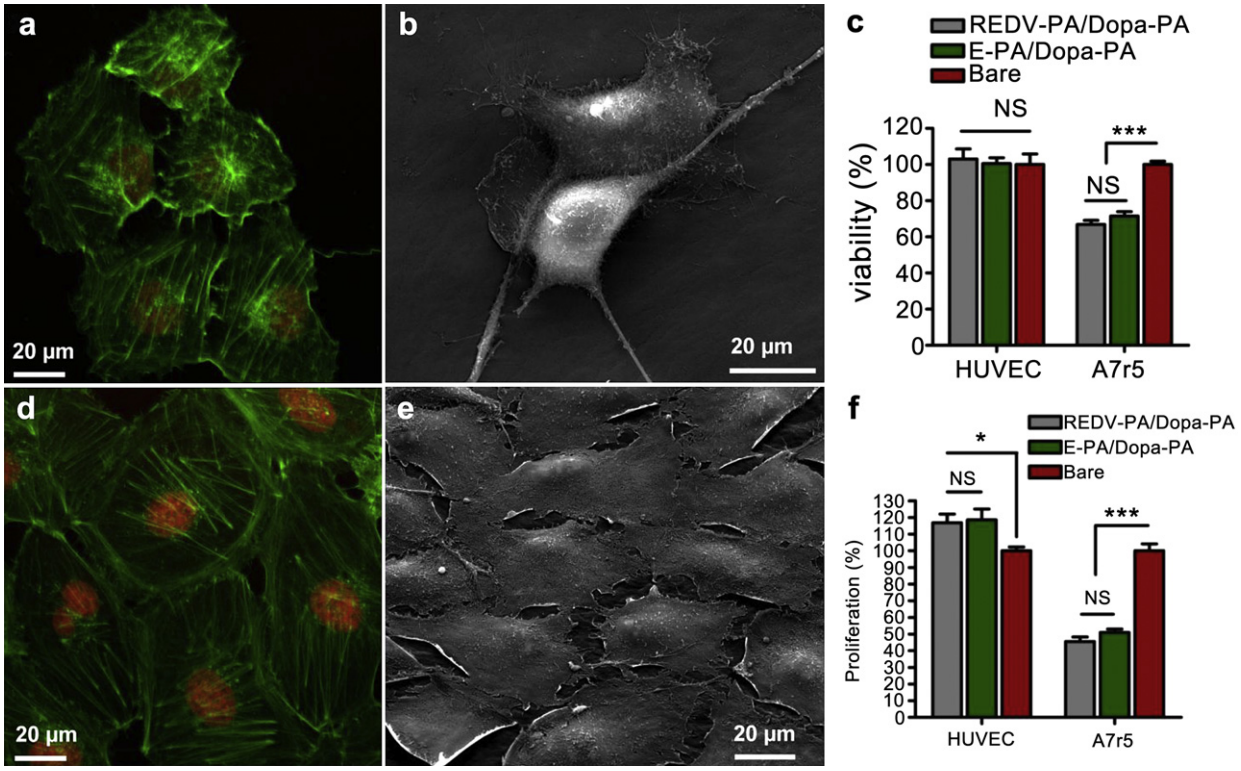

Fig. 5. Cellular morphology, viability and proliferation at 24 h and 72 h (a, b, d, e) HUVECs successfully maintained their native morphology and formed filamentous actin-based stress fibers after 24 and 72 h on REDV-PA/Dopa-PA network. (c) HUVECs were completely viable on both PA surfaces compared to the bare steel surface. On the other hand, A7r5 cells showed decreased viability on both PA coated steel surfaces compared to the bare steel surface. (f) HUVECs demonstrated enhanced proliferation on both PA coated surfaces while the proliferation of A7r5 cells decreased profoundly on the PA networks. a and d are confocal images. Green regions indicate filamentous actin stained by Phalloidin-TRITC, while red regions indicate the nucleus stained by TO-PRO®-3 iodide. b and e are SEM micrographs. $***p < 0.0001$, $*p < 0.05$, NS: No Significance.

surface, the recovery of endothelium is believed to regulate platelet activity inside the stent. However, it is still vital to evaluate the platelet attachment onto the bare stent coating because attachment of platelets at the implant site has been associated with thrombosis and subsequent restenosis [29]. We tested the attachment of platelets on PA coated stainless steel surfaces under static conditions at 2 h (Fig. 6). The number of platelets adhered on REDV-PA/Dopa-PA coated stainless steel surface was found to be 6.6 ± 0.87 folds higher with respect to bare stainless steel. However, relative adhesion of platelets on collagen I-coated surface was 70.5 ± 5.83 folds with respect to the bare surface, showing that adhesion of platelets on collagen I was more than 10 folds higher than PA

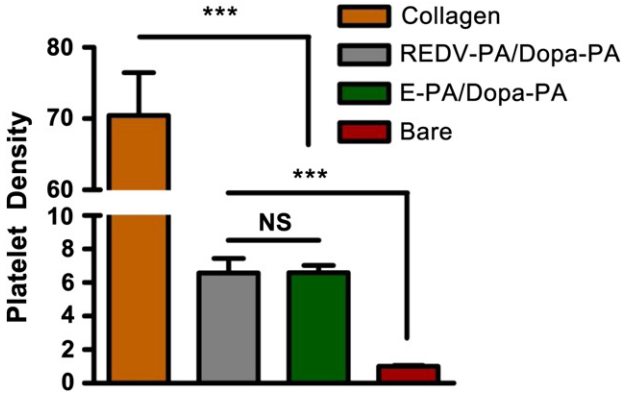

Fig. 6. The relative attachment of platelets on Collagen I, REDV-PA/Dopa-PA, and E-PA/Dopa-PA coated stainless steel surfaces with respect to bare steel surface at 2 h $***p < 0.0001$, NS: No Significance.

network. It was also noticed that there was no significant difference in attached platelet density between REDV-PA/Dopa-PA and E-PA/Dopa-PA, thereby indicating that REDV sequence by itself has no inhibition effect on platelet binding. REDV-PA/Dopa-PA network presents a promising feature in terms of relatively low platelet adhesion. Notably, rapid recovery of endothelial monolayer inside the stent surface will successfully prevent platelet binding and activation. In addition, peptide amphiphiles are known to be biodegradable owing to their peptide nature. It is believed that as the growing monolayer of endothelial cells synthesizes their native matrix, the PA coating will be degraded without leaving any known toxic degradation products. This feature of peptide nanofibers also encouraged us to conjugate REDV and Dopa residues on these nanostructures. Also, under *in vivo* shear conditions the coating might be worn off over time despite the anticorrosive feature of Dopa. However, these issues must be addressed in a separate discussion.

4. Conclusion

We developed a peptide-based self-assembled nanofibrous coating functionalized with fibronectin-derived endothelial cell specific adhesion signal, REDV, and mussel-adhesive protein inspired, Dopa residue. Functionalization of stainless steel surfaces with these bioactive molecules provided a native endothelium extracellular matrix-mimetic microenvironment that selectively promotes endothelial cell adhesion, spreading and proliferation. Strikingly, the results showed that the viability of vascular smooth muscle cells significantly decreased on the PA nanofibers. In addition, platelet attachment to the PA matrix in comparison to collagen I was found be significantly lower. These results show that our material provides

a promising approach for future clinical use as a bioactive coating for cardiovascular stents. Overall, our findings suggest that this peptide-based bioactive matrix can address major obstacles of contemporary stent technology by combining a biocompatible and convenient surface coating technology with integrin-mediated bioactivity that promote selective endothelialization on the stainless steel surface. These results provide vast opportunities for functionalization of currently used vascular grafts and coronary stents. The long-term success of stent implantation depends on the recovery of endothelium on the luminal surface of the stent. Endothelial cells carry out an indispensable mission in the proper functioning of the arteries and have a tight control over smooth muscle cell proliferation and platelet activity. Thus a treatment strategy to promote endothelialization around the wound site would prevent long term complications like restenosis and thrombosis.

Acknowledgments

We would like to thank Dr. A. Dana and Y. N. Ertas for their help in obtaining stainless steel sheets, Dr. U. Bagriacik for donating A10 cell line and Dr. M. Tosun for donating A7r5 cell line. We also would like to thank H. Ozturk and S. Ozkan for their technical help during *in vitro* work. We would like to express our gratitude to T.S. Erkal for AFM topography measurements, Z. Erdogan and M. Guler for their help in LC-MS and TEM. This project was supported by the Scientific and Technological Research Council of Turkey (TUBITAK) grant number 110M353 and COMSTECH-TWAS grant. H.C. is supported by TUBITAK BIDEB (2211) PhD fellowship. M.O.G. acknowledges support from the Turkish Academy of Sciences Distinguished Young Scientist Award (TUBA GEBIP).

Appendix. Supplementary data

Supplementary data related to this article can be found online at doi:10.1016/j.biomaterials.2011.08.018.

References

[1] Garg S, Serruys PW. Coronary stents: current status. J Am Coll Cardiol 2010; 56(10, suppl. 1):S1–42.
[2] Serruys PW, Strauss BH, Beatt KJ, Bertrand ME, Puel J, Rickards AF, et al. Angiographic follow-up after placement of a self-expanding coronary-artery stent. N Engl J Med 1991;324(1):13–7.
[3] van Domburg RT, Foley DP, de Jaegere PPT, de Feyter P, van den Brand M, van der Giessen W, et al. Long term outcome after coronary stent implantation: a 10 year single centre experience of 1000 patients. Heart 1999;82(suppl. 2):II27–34.
[4] Hoffmann R, Mintz GS, Dussaillant GR, Popma JJ, Pichard AD, Satler LF, et al. Patterns and mechanisms of in-stent restenosis: a serial intravascular ultrasound study. Circulation 1996;94(6):1247–54.
[5] Karas S, Gravanis M, Santoian E, Robinson K, Anderberg K, King 3rd S. Coronary intimal proliferation after balloon injury and stenting in swine: an animal model of restenosis. J Am Coll Cardiol 1992;20(2):467–74.
[6] Moses JW, Leon MB, Popma JJ, Fitzgerald PJ, Holmes DR, O'Shaughnessy C, et al. Sirolimus-eluting stents versus standard stents in patients with stenosis in a native coronary artery. N Engl J Med 2003;349(14):1315–23.
[7] Daemen J, Ong ATL, Stefanini GG, Tsuchida K, Spindler H, Sianos G, et al. Three-year clinical follow-up of the unrestricted use of sirolimus-eluting stents as part of the rapamycin-eluting stent evaluated at rotterdam cardiology hospital (RESEARCH) registry. Am J Cardiol 2006;98(7):895–901.
[8] McFadden EP, Stabile E, Regar E, Cheneau E, Ong ATL, Kinnaird T, et al. Late thrombosis in drug-eluting coronary stents after discontinuation of antiplatelet therapy. Lancet 2004;364(9444):1519–21.
[9] Finn AV, Joner M, Nakazawa G, Kolodgie F, Newell J, John MC, et al. Pathological correlates of late drug-eluting stent thrombosis. Circulation 2007; 115(18):2435–41.
[10] Awata M, Kotani J-i, Uematsu M, Morozumi T, Watanabe T, Onishi T, et al. Serial angioscopic evidence of incomplete neointimal coverage after sirolimus-eluting stent implantation. Circulation 2007;116(8):910–6.
[11] Hubbell JA, Massia SP, Desai NP, Drumheller PD. Endothelial cell-selective materials for tissue engineering in the vascular graft via a new receptor. Nat Biotechnol 1991;9(6):568–72.
[12] Massia SP, Hubbell JA. Vascular endothelial cell adhesion and spreading promoted by the peptide REDV of the IIICS region of plasma fibronectin is mediated by integrin alpha 4 beta 1. J Biol Chem 1992;267(20):14019–26.
[13] Lee H, Dellatore SM, Miller WM, Messersmith PB. Mussel-inspired surface chemistry for multifunctional coatings. Science 2007;318(5849):426–30.
[14] Lee H, Scherer NF, Messersmith PB. Single-molecule mechanics of mussel adhesion. Proc Natl Acad Sci U S A 2006;103(35):12999–3003.
[15] Fant C, Hedlund J, Höök F, Berglin M, Fridell E, Elwing H. Investigation of adsorption and cross-linking of a mussel adhesive protein using attenuated total internal reflection fourier transform infrared spectroscopy (ATR-FTIR). J Adhes 2010;86(1):25–38.
[16] Fant C, Sott K, Elwing H, Hook F. Adsorption behavior and enzymatically or chemically induced cross-linking of a mussel adhesive protein. Biofouling 2000;16(2–4):119–32.
[17] Hartgerink JD, Beniash E, Stupp SI. Self-assembly and mineralization of peptide-amphiphile nanofibers. Science 2001;294(5547):1684–8.
[18] Silva GA, Czeisler C, Niece KL, Beniash E, Harrington DA, Kessler JA, et al. Selective differentiation of neural progenitor cells by high-epitope density nanofibers. Science 2004;303(5662):1352–5.
[19] Kushwaha M, Anderson JM, Bosworth CA, Andukuri A, Minor WP, Lancaster Jr JR, et al. A nitric oxide releasing, self assembled peptide amphiphile matrix that mimics native endothelium for coating implantable cardiovascular devices. Biomaterials 2010;31(7):1502–8.
[20] Tysseling-Mattiace VM, Sahni V, Niece KL, Birch D, Czeisler C, Fehlings MG, et al. Self-assembling nanofibers inhibit glial scar formation and promote axon elongation after spinal cord injury. J Neurosci 2008;28(14):3814–23.
[21] Baudin B, Bruneel A, Bosselut N, Vaubourdolle M. A protocol for isolation and culture of human umbilical vein endothelial cells. Nat Protoc 2007;2(3): 481–5.
[22] Srinivasan R, Marchant RE, Gupta AS. In vitro and in vivo platelet targeting by cyclic RGD-modified liposomes. J Biomed Mater Res 2010;93A(3):1004–15.
[23] Niece KL, Hartgerink JD, Donners JJJM, Stupp SI. Self-assembly combining two bioactive peptide-amphiphile molecules into nanofibers by electrostatic attraction. J Am Chem Soc 2003;125(24):7146–7.
[24] Fischell TA. Polymer coatings for stents: can we judge a stent by its cover? Circulation 1996;94(7):1494–5.
[25] Chung T-W, Liu D-Z, Wang S-Y, Wang S-S. Enhancement of the growth of human endothelial cells by surface roughness at nanometer scale. Biomaterials 2003;24(25):4655–61.
[26] Wu Y, Zitelli JP, TenHuisen KS, Yu X, Libera MR. Differential response of Staphylococci and osteoblasts to varying titanium surface roughness. Biomaterials 2011;32(4):951–60.
[27] Salloum DS, Olenych SG, Keller TCS, Schlenoff JB. Vascular smooth muscle cells on polyelectrolyte multilayers: hydrophobicity-directed adhesion and growth. Biomacromolecules 2004;6(1):161–7.
[28] Ashwini R, Thomas JW. Increased endothelial cell adhesion and elongation on micron-patterned nano-rough poly(dimethylsiloxane) films. Nanotechnology 2009;20(30):305102.
[29] Joner M, Finn AV, Farb A, Mont EK, Kolodgie FD, Ladich E, et al. Pathology of drug-eluting stents in humans: delayed healing and late thrombotic risk. J Am Coll Cardiol 2006;48(1):193–202.